

**MODELING THE SEASONAL SOUTH POLAR CAP SUBLIMATION RATES AT DUST STORM CONDITIONS.** B. P. Bonev<sup>1</sup>, P. B. James<sup>1</sup>, M. J. Wolff<sup>2</sup>, J.E. Bjorkman<sup>1</sup>, G. B. Hansen<sup>3</sup>, and J. L. Benson<sup>1</sup>, <sup>1</sup>Ritter Astrophysical Research Center, Dept. of Physics and Astronomy, Univ. of Toledo, Toledo, OH 43606, USA (bbonev@kuiper.gsfc.nasa.gov; pbj@physics.utoledo.edu; jon@physics.utoledo.edu; jben-son@physics.utoledo.edu), <sup>2</sup>Space Science Institute, 3100 Marine Street, Boulder, CO 80303-1058, USA (wolff@colorado.edu), <sup>3</sup>Planetary Science Institute, Northwest Division, Univ. of Washington, Seattle laboratory, Seattle, WA 98195 (ghansen@rad.geology.washington.edu).

**Introduction:** Carbon dioxide is the principal component of the Martian atmosphere and its interaction with the polar caps forms the CO<sub>2</sub> seasonal cycle on the planet. A significant fraction of the atmospheric constituent condenses on the surface during the polar winter and sublimates back during spring. The basic aspects of the CO<sub>2</sub> cycle have been outlined by Leighton and Murray [1] and a number of follow-up theoretical models ranging from energy balance to general circulation models have been used to study the physical processes involved in the cycle [2,3].

Observations of the boundaries of the seasonal CO<sub>2</sub> caps and the pressure curves measured by the Viking landers have been used to search for interannual variability in the carbon dioxide cycle. An important aspect of these studies is the lack of evidence for a strong coupling between the Martian dust cycle and the CO<sub>2</sub> cycle. Ground-based historical data suggests some connection, but disentangling real differences from systematic errors is problematic [4]. On the other hand, the Viking pressure curves for years with vastly different dust storm histories have showed only subtle differences [2].

**MGS Observations:** The 1999 and 2001 spring regressions of the south seasonal polar cap have been observed in unprecedented detail by MGS in both visual (MOC) and IR (TES) wavelengths. This has provided an excellent opportunity for a precise comparison between the cap regression rates for years with very different atmospheric conditions in early spring. While the early phase of the 2001 regression occurred during a global dust storm [5], the 1999 season was significantly less dusty. It should be emphasized that the MGS observations allow studies not only of the average cap decay but also of localized regions with distinctive albedo properties, such as the Cryptic region [6] (low visual albedo) and the Mountains of Mitchel [6,7] (high visual albedo). A schematic representation of the main observational results is shown on Figure 1:

1. Low visual albedo regions displayed slower regression (by  $L_s \sim 4^\circ - 5^\circ$ ) in 2001 compared to 1999 [6].
2. Bright regions showed faster regression rates by the same amount [6,7].

3. Our preliminary average regression curves for 2001 and 1999 are very similar despite the very different dust storm history.

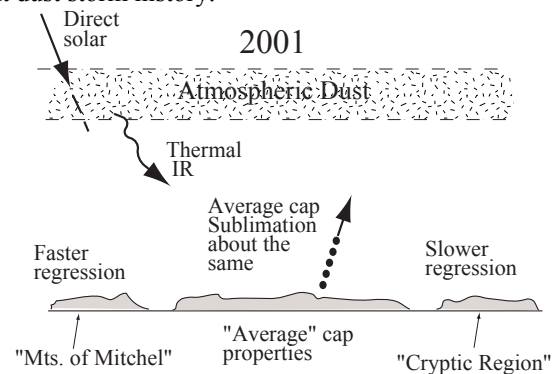


Figure 1. A schematic summary of the MGS observations of the 2001 south polar cap decay. MOC images show that a significant fraction of the cap was obscured by dust in early spring. The regression rates are compared qualitatively to the 1999 season. Dark areas displayed slower decay [6], while areas with high visual albedo regressed faster than in 1999 [6,7].

**Modeling the CO<sub>2</sub> Frost Sublimation As a Function of the Atmospheric Dust Load:** The three types of surface responses to increased atmospheric dust have been predicted using a radiative transfer model through a dusty atmosphere bounded by a sublimating CO<sub>2</sub> surface. The basic model has been described in [7]. These are monte carlo calculations which use the condition of radiative equilibrium and year-to-date dust single scattering properties for both visual and IR wavelengths [8]. The model considers two effects of dust: *atmospheric dust* which redistributes the radiation incident to the surface from visual frequencies to the IR, and *surface dust intermixed in the frost*, which is the main factor determining the surface albedo spectrum [9]. Pure CO<sub>2</sub> frost has a high visual albedo and a distinct minimum in the IR emissivity near 25  $\mu\text{m}$ . Intermixed dust on the surface tends to lower significantly the visual albedo and to bring the IR emissivity close to unity. The second important surface parameter is the grain size of the CO<sub>2</sub> frost.

While in [7] we have considered only the limiting cases of very high and very low visual albedos, here we present a detailed parameter study spanning various dust-to-ice mixing ratios and frost grain sizes. The results are shown in Figure 2a-2c which plots the CO<sub>2</sub>

sublimation flux (SF) versus the total atmospheric dust optical depth at 550 nm. The SF has been normalized to the total flux incident on the atmosphere and calculated as a difference between the spectrally integrated fluxes absorbed and emitted by the surface (set to sublimate at 147 K).

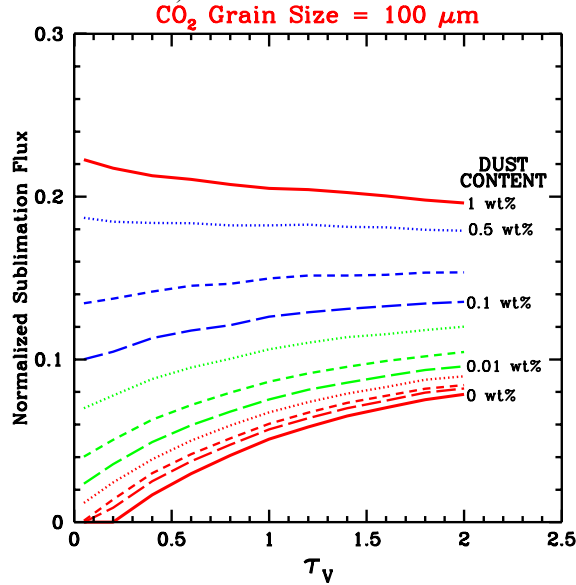


Figure 2a. CO<sub>2</sub> Sublimation Flux vs. Total Atmospheric Dust Optical Depth at 550 nm for a frost grain size of 100 μm and various contents of intermixed surface dust.

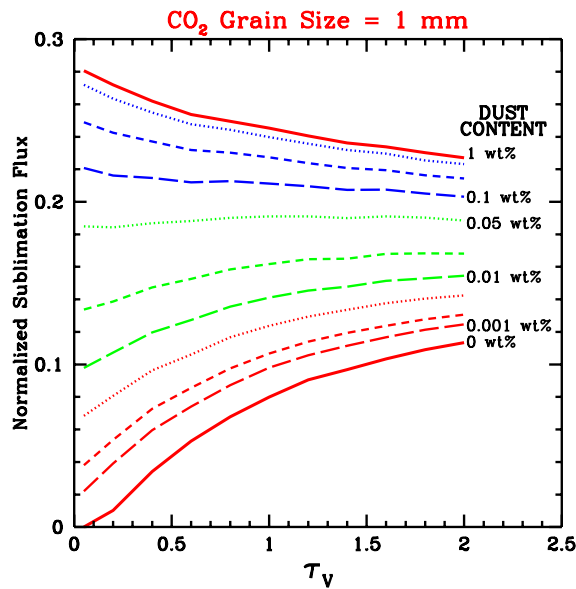


Figure 2b. CO<sub>2</sub> Sublimation Flux vs. Total Atmospheric Dust Optical Depth at 550 nm for a frost grain size of 1 mm and various contents of intermixed surface dust.

The main model results reproduce qualitatively the observations presented schematically on Figure 1:

1. The absorption of surface frost with a high dust content (1 wt% being the upper limit [9]) is dominated by visual photons. Therefore the attenuation of direct

solar radiation by atmospheric dust results in retarded sublimation.

2. Conversely, the absorption of regions with low dust content is dominated by IR photons, owing to the high visual albedos. In this case the visual-to-IR redistribution of the energy incident to the surface, caused by atmospheric dust, leads to increased sublimation rates.

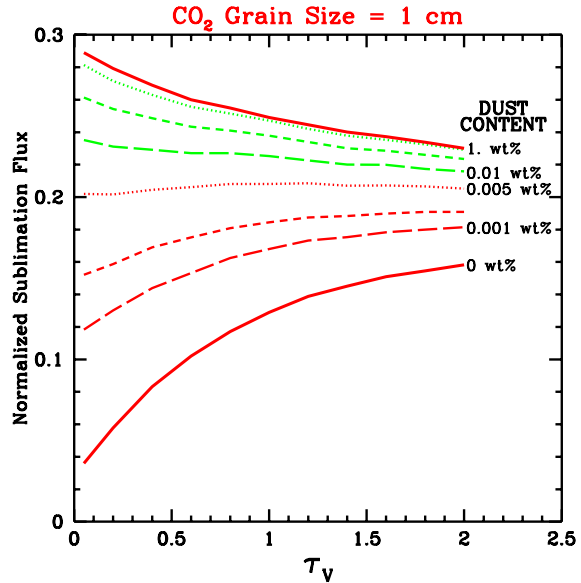


Figure 2c. CO<sub>2</sub> Sublimation Flux vs. Total Atmospheric Dust Optical Depth at 550 nm for a frost grain size of 1 cm and various contents of intermixed surface dust.

3. There is a wide range of combinations between surface dust content and frost grain size for which the CO<sub>2</sub> sublimation rates show only subtle variations with the amount of atmospheric dust load. In these cases the surface absorption is distributed equally between visual and IR wavelengths, so the overall atmospheric dust effect is not important. It should be emphasized that the discussed region of the parameter space represents a "typical frost" [9] and consequently explains the apparent insensitivity of the *average decay rate* of the south seasonal cap to dust storm activity. Strong coupling between sublimation and atmospheric dust exists primarily on *local scale* for regions with "deviant" surface albedos.

A note should be made about the possibility that newly deposited surface dust played a role in the faster regression of bright regions (like the Mountains of Mitchel) by lowering the surface albedo and thus increasing the absorbed flux and consequently the sublimation rate. While this scenario cannot be ruled out, it fails to explain the slowing down of the dark regions such as the Cryptic region, which is consistent with the effect of atmospheric dust.

**Modeling improvements:**

*Surface properties.* The surface albedo is a major parameter and its accurate modeling is of primary importance. Compared to our first limiting case study [7] we have examined in depth the albedo changes with surface dust-to-ice mixing ratio and frost grain size; the variation of the albedo with photon incident angle and the dependence on the ratio of direct/diffuse incident radiation have been included. In monte carlo calculations the albedo dependence on the direction of the reflected photons is also important. This variable has been held as a free parameter by simulating different laws of surface reflection. A good constraint of the best directional distribution of the photons reflected would enable incorporating this factor accurately into our model.

*Atmospheric radiative transfer.* The results presented are based on radiative transfer through atmospheric dust. The successful interpretation of all observations with this model is primarily due to the fact that (1) the surface boundary conditions include sufficient detail, and (2), that the radiative equilibrium calculations are fairly good in representing the visual-to-IR redistribution of incident photons caused by atmospheric dust. At the same time an improved accuracy and wider applicability is achievable only by including the CO<sub>2</sub> 15 μm band as a second opacity source. Using well-constrained dust single scattering properties enables fairly accurate calculations in the visual, but in the IR the CO<sub>2</sub> band "screens" part of the thermal dust emission (and vice versa). This interaction can be represented accurately only if these two opacity sources are considered together.

The challenge is that our monte carlo calculations use the condition of radiative equilibrium, i.e. the atmospheric temperature profiles are not used as input but have been calculated based on the opacity sources given. The original algorithm [10] was built for temperature-independent opacity sources like dust, and for this case the whole procedure is non-iterative. The gas opacity is temperature and pressure dependent, and therefore its inclusion causes a major change in the model. Addressing this, we first calculated the CO<sub>2</sub> extinction coefficients averaged over parts of the 15 μm band using the correlated-k approach [11]. This allowed the building of a simple "dust-and-gas" model in which the CO<sub>2</sub> opacity is calculated for some "characteristic" pressure and temperature. The next step has been (April 2003) developed, and it includes self-consistent calculations in which the gas opacity varies with altitude through pressure and temperature. Ultimately such modeling can be used outside the polar conditions to accurately simulate radiative effects during global dust storms.

**Acknowledgement:** Five of the authors (BPB, MJW, PBJ, GBH, and JLB) were supported by grants from the Mars Data Analysis Program. JEB was supported by NSF Grant AST-9819928.

**References:** [1] Leighton, R. B. and Murray, B. C. (1966) *Science*, 153, 136–144. [2]. James, P. B. et al. (1992) In *Mars*, 934-968. [3]. James, P. B. et al. (2003) *Adv. Sp. Res.*, in press. [4]. James, P. B. et al. (1987) *Icarus*, 71, 298-305. [5] Smith, M. D. et al (2002) *Icarus*, 157, 259-263. [6] Titus, T. N. and Kieffer, H. H. (2002) *LPS XXXIII*, #2071. [7] Bonev, B. P. et al. (2002) *GRL*, 29, 2017, doi:10.1029/2002GL015458. [8] Wolff, M J. and Clancy, R. T. (2003) *JGR*, in press. [9] Hansen, G. B. (1999) *JGR*, 104, 16,471-16,486. [10] Bjorkman, J. E. and Wood, K. W. (2001) *ApJ*, 554, 615-623. [11] Goody, R. et al. (1989) *JQSRT*, 43, 191-199.